Dimensional considerations on the mechanical properties of 3D printed polymer parts

Nabila Elmrabet[1], Petros Siegkas[1]

[1] Department of Engineering, Nottingham Trent University, Clifton, Nottingham, NG11 8NS, UK,

Abstract

Additive manufacturing offers a useful and accessible tool for prototyping and manufacturing small volume functional parts. Polylactic acid (PLA) and thermoplastic polyurethane (TPU) are amongst the most commonly used materials. Characterising 3D printed PLA and TPU is potentially important for both designing and finite element modelling of functional parts. This work explores the mechanical properties of additively manufactured PLA/TPU specimens with consideration to design parameters including size, and infill percentage. PLA/TPU specimens are 3D-printed in selected ISO standard geometries with 20%, 60%, 100 % infill percentage. Tensile and compression test results suggest that traditional ISO testing standards might be insufficient in characterising 3D printed materials for finite element modelling or application purposes. Infill percentage in combination to design size, may significantly affect the mechanical performance of 3D printed parts. Dimensional variation may cause inhomogeneity in mechanical properties between large and small cross section areas of the same part. The effect was reduced in small cross section parts where reducing the nominal infill had less effect on the resulting specimens. The results suggest that for 3D printed functional parts with significant dimensional differences between sections, the material properties are not necessarily homogeneous. This consideration may be significant for designers using 3D printing for applications, which include mechanical loading.

Keywords: 3D Printing, 3D printed material characterisation, Infill Percentage, PLA, TPU, ISO standard, dimensional variation

1. Introduction

Additive Manufacturing (AM), also known as 3D printing (3DP), can be cost effective, by comparison to subtractive manufacturing, as a result of the reduction in waste material and the capacity to produce complex geometries (Brenken, et al. 2018). Many AM techniques such as stereo-lithography (SLA), selective laser sintering (SLS), and fused filament fabrication (FFF) have been developed to process different materials (Han, et al. 2019). However, FFF, also known as fused deposition modelling (FDM) process, is a popular example of AM methods developed in the late 1980s (Guo and Leu 2013). FDM is

a rapid solid-based prototyping technology used to produce complex geometry parts (Pahonie, et al. 2017, Bin Ishak, Fleming and Larochelle 2019). The FDM process is based on computer guided deposition of molten feed stock material (Cantrell, et al. 2017). FDM works by adding and joining materials together without requiring a template or mould (Chen, et al. 2017). The FDM method is increasingly used to fabricate customized products for engineering as well as medical applications (Brenken, et al. 2018).

Typically, the X- and Y-axes lies on the horizontal plane, and the 3D build platform travels vertically along the Z-axis (Rohde, et al. 2018). The target parts are fabricated by extruding a semi-liquid material from the original filament through a heated nozzle in a prescribed pattern and onto a platform (Yao, et al. 2019). As the material is deposited, it cools, solidifies and bonds with the adjoining material (Mani, Lyons and Gupta 2014). Complex geometries may need support material to enable the generation of geometric overhangs (Brenken, et al. 2018). More complex systems include multiple nozzles which can deposit different materials (Guo and Leu 2013).

Thermoplastic materials such as Poly Lactic acid (PLA) and Polyurethane (TPU) are amongst the most common (Sha, et al. 2016). Biodegradable polymers have been widely considered as a more environmentally friendly option by comparison to conventional polymers. PLA is part of the synthetically prepared aliphatic polyesters family, which can be derived from renewable resources such as sugar, corn, potato and other products (Sha, et al. 2016, Treiser, et al. 2013). PLA is considered as biodegradable thermoplastic polyester and non-toxic. It has a relatively low melting point (160-170°C) and low shrinkage rate (Fernández-Vicente and Conejero 2016). It is biocompatible when in contact with living tissues making it suitable for bone scaffolds, structures, and drug capsulations (Avérous 2008). In addition to elimination of need to remove implants, the products of degradation process of PLA usually include water and carbon dioxide which can be naturally disposed of by the human body. These characteristics make PLA one of the most popular material for FDM 3D printing (Dal Maso and Cosmi 2018). Nevertheless, pure PLA material has limited applications due to the limitations of its mechanical properties (Sha, et al. 2016). PLA is considered brittle with low toughness, impact strength, and flexibility (Tao, Y., et al. 2019).

TPU is a highly linear elastic polymer composed of soft parts in form of flexible polyester or polyether, and hard parts which usually diisocyanates with benzyl structure (Chen, et al. 2017). The main characteristics of TPU include good abrasion resistance, high elongation, moderate tensile and compression strength, and good biocompatibility (de Leon, et al. 2016). These properties enable TPU to be commonly used in different fields, including tissue engineering, coatings, adhesives and foaming. Limitations of TPU are the poor shape fixity and low mechanical strength (Chen, et al. 2017).

FDM offers a flexible and a relatively simple manufacturing method which makes it attractive to various fields. Polymeric scaffolds with deliberately designed geometrical features (i.e. size, porosity, and interconnectivity) can benefit cell growth (Chen, et al. 2017) and bioresorbable implants can assist in reconstructive surgery (Hofmann, Kluger and Fische 1997). Highly stretchable sensors can be 3D-printed into devices, allowing integration of soft functional material to be used in soft robotics, wearable electronics, and human/machine interfaces (Muth, et al. 2014). Prosthetic limbs can be customised using FDM, however it is difficult for any design alone to perform all the several functions of replaced limbs and suitably satisfy unique application requirements (Tao, Z., et al. 2017).

Manufacturing 3D printed functional products requires a clear understanding of the mechanical properties of 3D printed parts (Bin Ishak, Fleming and Larochelle 2019). The mechanical properties of 3D printed parts tend to be different than those of parts that were produced by conventional methods (e.g. homogeneous injection moulding) (Song, et al. 2017, Kim, et al. 2017). The practical use of FDM produced parts is generally limited to applications with low mechanical loading requirements (Mani, Lyons and Gupta 2014). Nevertheless the mechanical properties of 3D printed lightweight cellular composite structures, can be controlled by controlling the design and print process that can affect their elastic properties and strength (Compton and Lewis 2014).

Efforts to control properties of 3D-printed parts include considering alteration of different printing parameters such as printing orientations, layer height, material type, printing speed, number of perimeter wall (Pei, et al. 2015), infill pattern, raster angle, infill density, air gap sizes, and printing temperatures (Parandoush and Lin 2017).

Tensile properties were studied by Ebel and Sinnemann (2014) for PLA and ABS as function of infill pattern and infill density. They found that completely filled PLA had higher yield strength and young's modulus of 42 MPa and 2.6 GPa than the 32 MPa and 1.9 GPa of ABS. From their observation they concluded that the combination of PLA and line pattern (100% infill) should be chosen for high resistance against deformation while ABS and line pattern led to relatively ductile parts.

Torres et al. (2015) experimentally investigated the link between the layer thickness, infill density, and post-processing heat-treatment time at 100°C on the mechanical shear properties of 3D-printed PLA. Their conclusion indicated that the combination of high (100%) infill density and 0.1 mm layer thickness is desired to achieve maximum values of material properties.

In another study, Torres et al. (2016) also considered layer thickness, infill direction, infill density, extrusion temperature and printing speed to obtain the heights PLA strength and durability. Their results showed that an optimisation of settings can be pursuit in order to yield high performance for general material properties. They deduced that infill density is the most influential parameter for both optimal tensile and fracture properties. Other parameters, such as 0.1 mm layer thickness, 230°C extrusion temperature, 60-90 mm/s printing speed and 90/180° infill direction, are also preferred for the best tensile performance.

Qattawi et al. (2017) used experiment and computational methods to study a variety of processing parameters that were independently investigated to establish their effect on the mechanical properties and dimensional accuracy of 3D printed parts. They concluded that the mechanical properties are not highly affected by the infill pattern or the printing speed due to the down-sizing geometry of specimens. Nevertheless, the infill percentage lead to better mechanical performance. The building direction, extrusion temperature and layer height are parameters that need to be adjusted in order to improve the dimensional accuracy of 3D printed parts. Kim et al. (2017) also investigated the effect of the orientation angle, infill rate and material type on the tensile strength of PLA and ABS, and found that PLA printed in x-direction with 100% infill exhibit the best mechanical properties for single material. Their study also indicated that the efficiency of mechanical properties can be enhanced by the structural design of multiple material parts, even if the materials ratio is kept constant.

Li et al. (2018) considered, three major process parameters, including layer thickness, deposition velocity and infill rate. The experiments were in relation to tensile strength. The experimental and simulation results indicated that layer thickness plays the main role in altering the interface bonding and hence the tensile strength, followed by deposition speed, and infill density.

Hohimer et al. (2017) studied the tensile properties of FDM thin walled TPU as a function of nozzle temperature (190°, 205°, 220°), raster angle (0,45°,90°) and air gaps (-0.05, +0.05mm). They concluded that air gaps had a significant effect on the ultimate tensile strength (UTS) while temperature and raster pattern were less significant. However, the raster pattern was significant with a large enough air gaps. In their study, it was found that TPU parts printed with a negative air gap of -0.05 mm have isotropic mechanical properties.

A benefit in the use of 3D printed PLA and flexible polymers (TPU, ABS) is that they can be tailored, in terms of their properties, to satisfy applications needs. Pahonie et al. (2017) studied the effect of different mesh densities on the mechanical properties of 3D printed

ABS and PLA specimens for orthotic device. They concluded that various mesh densities for different areas of an orthotic device (insole) would help off-lead up to 25% alleviating the foot stress. They found that the highest strength of PLA specimens, recorded at 44.24 MPa, are in good agreement with the numerical results obtained by ANSYS software simulation with finite elements of a 3D printed insole. They conclude that varying mesh density can help alleviating up to 25% of the foot stress.

The studies mentioned above have mainly investigated the optimal printing parameters on the quality of 3D printed parts. Some filament manufacturers provide some data for their filament materials (prior to printing). However, there seems to be a lack of sufficient testing standards for 3D printed materials (Popescu, et al. 2018). Furthermore there is limited information on the variability of properties based on design parameters, i.e. part dimensions. Even if all 3D printing parameters are kept nominally constant for a specific part, the mechanical properties are not necessarily homogeneous. Parts that are designed to have large dimensional differences e.g. small and large cross sections, may exhibit significant differences in the material properties between those regions. This is a consideration to be addressed in designing or modelling functional parts that are intended for manufacturing using FDM techniques. This study highlights this effect, by investigating the effect of infill density, on the mechanical properties of PLA and TPU 3D printed specimens of different dimensions.

2. Materials and Methods:

The aim of this study is to examine the mechanical performance of PLA and TPU95A samples in relation with infill percentage and specimen dimensions. Commercial PLA (RS PRO-∅ 2.85 mm) and TPU95A (Ultimaker-∅2.85 mm) filaments were tested.

2.1. Dimension of specimens and printing parameters

PLA and TPU specimens of different sizes and infill percentages were manufactured. The effects of infill and dimension on the variation of mechanical properties were examined.

Tensile and compressive testing:

Tensile dogbone PLA specimens were 3D printed in accordance to ISO-527 Types 1A & 1B, and ISO 37:2017 Type 2 (Figure 1). These specimen standards were chosen in order to explore the dimensional effects in sections of parts where discrepancy between nominal to actual infill percentage might be significant. The second batch of tensile test specimens were of TPU 95A and 3D-printed in accordance to ISO 527-2 Type 1A specimen standards. Cylindrical PLA specimens were used for compression tests (Table 3).

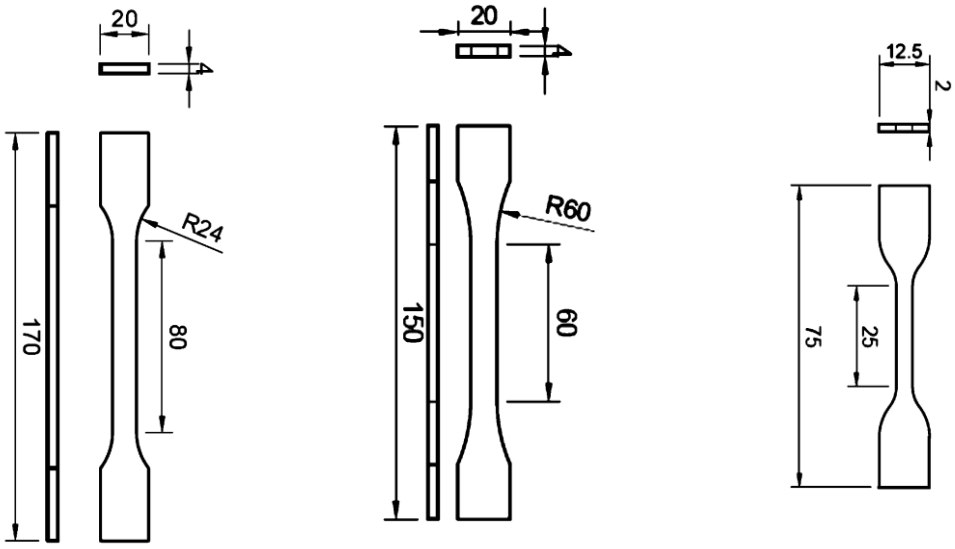

Figure 1 Sketch of ISO-527 specimens Types 1A & 1B and ISO-37 specimens Type 2

Specimens were designed using Autodesk Fusion 360 software and exported in Stereo-lithography (STL) file format. They were then imported into Cura 3.2.1 software and prepared for 3D printing in G-code format. The tensile and compressive specimens were fabricated on an Ultimaker 3 FDM 3D printer using a 0.4 mm nozzle diameter. The tensile specimens were printed lying flat in the X direction and the compression specimens in the standing position (such that Z aligned with the cylinder axis).

In both tensile and compression tests, the effect of infill on the mechanical properties of PLA and TPU95A was evaluated. Three different infill percentages were considered (20%, 60%, 100%). Other parameters such as layer height, print core, air gap, print speed and temperature were kept constant. Setup and control parameters are listed in Table 1.

Table 1 Setup parameters for each sample used in the study

Parameter	PLA	TPU 95A
Layer height (mm)	0.1	0.1
Print core (nuzzle) size (mm)	AA 0.4	AA 0.4
Print speed (mm/s)	70	25
Travel speed (mm/s)	250	300
Liquified temperature (°C)	200	223
Brim width (mm)	7.0	8.75
Filament colour	Red	White
Material	RS PRO 1.75 mm	Ultimaker 2.85 mm

2.2 Uniaxial Mechanical testing (machine and conditions)

Testing was performed on a SHIMADZU AG-X plus screw driven machine, equipped with a 50 kN load cell. The specimens were subjected to uniaxial tension/compression until failure or 20% strain. Each test was repeated three times. Sample position is shown in Figure 2 (a). Specimens were marked at the grips, prior to testing, in order to visually identify any slippage. Displacement was digitally recorded using a non-contact TRViewX high performance extensometer (absolute accuracy ±1.5 μm). Filaments and specimens were kept at room temperature and at approximately 40% relative humidity for more than 24 hours. Specimens were tested at room temperature and at 10^{-4} s^{-1} strain rate (Table 2).

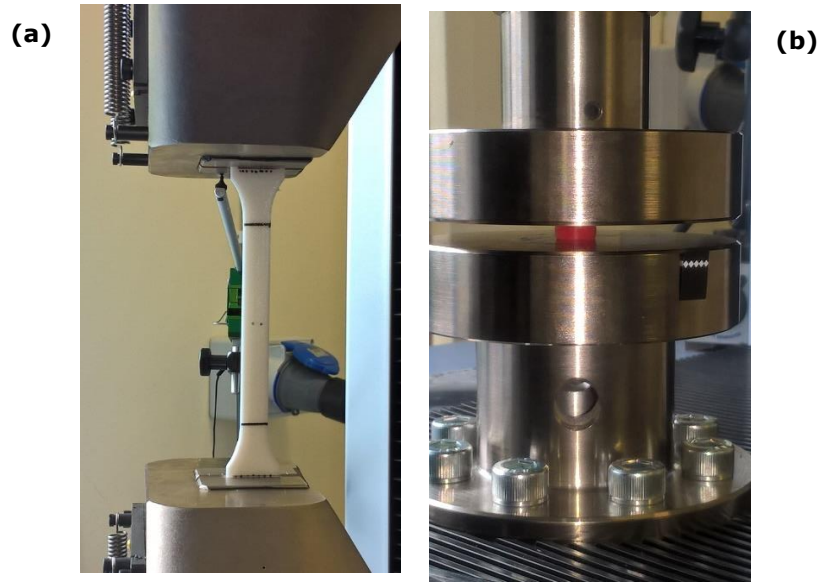

Figure 2 Mechanical testing of specimens(a) Tensile test specimen of TPU (ISO-527 Type 1A), (b) Compression test specimen of PLA.

Table 2 Test speed of Tensile test specimens for both series 1 (PLA) and series 2 (TPU)

Sample ISO	Type	GL (mm)	Test speed (mm/min)
527-2	1A	75	0.45
527-2	1B	50	0.30
37:2003	2	20	0.123

Table 3 Test speed of Compression test specimens of PLA only

Sample Dimension D (mm)	H(mm)	Test speed (mm/min)
10	10	6.104
5	5	3.428

Compression specimens were tested at 10^{-2} s^{-1} strain rate (Figure 2 (b)). Stroke displacement was corrected using the measured machine compliance. Cylindrical specimens of 10 mm and 5 mm diameter were 3D printed at infill percentages of 20%, 60%, 100%, and 20 %, 60 % correspondingly. Table 3 summarises specimen dimension and test speed of compression test for PLA specimens.

MATLAB code was used for analysis. The tensile and compression modulus (E_t, E_c) for tested specimens were determined considering the linear part of the stress–strain curve and the slope was estimated by a linear fit. Each test was repeated at least three times. All quantitative data are reported as the mean ± standard deviation values.

3. Results and Discussion

3.1. *Tensile Test of PLA and TPU*

Figure 3 shows the stress strain curve results for, PLA and TPU tensile tests. All PLA specimens reached maximum tensile stress for less than 5% strain. Ultimately specimens failed after necking. No significant difference was observed between ISO-527 type 1A and 1B. The effects of increasing the infill settings to stress response doesn't follow a linear relation. The effect of increasing the infill from 20 to 60% on the stress response, seemed to be smaller than that from 60 to 100%. ISO-37 PLA specimens at 20 % infill seemed to behave similarly to ISO-527 at 100% infill. This would suggest that infill settings variation has less effect in smaller sample geometries. Possibly the outlining walls of the smaller cross section specimen (i.e. ISO-37) are proportionally larger than that of a large cross section specimen i.e. ISO-527, and therefore resulting in a higher overall density, closer to 100%. Infill effects are limited by printer resolution and specimen cross section size.

Necking effects for PLA ISO 527 specimens seemed more localised for lower infills. T37 specimens showed significantly higher ductility for constant stress and continued to elongate beyond 100% strain. Drawing effects (Davis 2004) were significantly more prominent in the smaller cross-sectioned specimen.

The PLA ISO 527 average values of the elastic modulus (E_t), ultimate tensile strength (σ_t), and elongation at break point (ε_b), extracted from the curves are tabulated in Table 4 and compared to published values. A crucial factor in the design process of manufactured parts is the ultimate strength (σ_t) (Pei, et al. 2015). As shown in Table 4 the average values of ultimate strength of 20% infill ISO 37 Type 2 specimens are the highest, of 47.08±1.8 MPa followed by the 100% infill of bigger sized ISO 527 Type 1A and 1B specimens of 44.70±0.1 MPa and 43.82±0.8 MPa, respectively. These results were in agreement with those reported in literature for PLA printed under different parameters and conditions (Pei, et al. 2015, Chacón, et al. 2017). Particularly, the difference in performance of ISO 37 type 2 (20% infill) appears increased E_t (4.07±1.02 GPa) as compared to other specimens of varied size and infill. This highlights the ductile behaviour with significant plastic deformation of PLA small printed parts. The data suggests that model geometry had a significant influence on the strength and elastic properties despite the intended infill

density in 3D printed small parts. This was possibly a result of the printing method and resolution limitations of the 3D printer.

Larger parts with reduced infill (i.e. Type 1A and 1B samples, with 20% and 60% infill) would result in big gaps from at which damage can start and propagate (Wu, et al. 2015). Large specimens with 100% infill or small specimens, would result in cross-linked extruded lines of bonded material that would result in significantly higher strength.

Table 4 Overview mechanical properties of PLA and TPU as a function of infill percent (mean±SD, n=3).

Specimen ID	Infill 20 %			Infill 60 %			Infill 100%		
	σ_t MPa	E_t GPa	ε_b %	σ_t MPa	E_t GPa	ε_b %	σ_t MPa	E_t GPa	ε_b %
T527-1A	28.51 ±0.7	2.11 ±2.01	0.03 ±0.01	31.32 ±0.1	1.93 ±1.89	0.04 ±0.01	44.70 ±0.1	2.62 ±0.34	0.14 ±0.02
T527-1B	29.38 ±0.6	2.03 ±0.4	0.05 ±0.01	31.53 ±0.8	2.11 ±0.67	0.06 ±0.02	43.82 ±0.8	2.98 ±0.61	0.30 ±0.08
T37-2	47.08 ±1.8	4.07 ±1.02	-	-	-	-	-	-	-
Typical Range (Tao, Z., et al. 2017, Pei, et al. 2015, Subeshan, et al. 2018, Tymrak, Kreiger and Pearce 2014)	σ_t (MPa) = 15.5-72.2			E_t (GPa) = 2.02-4.0			ε_b (%) = 0.5-9.2		

Figure 3 shows the typical stress-strain behaviour of flexible TPU. Results were very repeatable. The overall stress-strain trends for all the infill percent were similar, with the higher infill percent specimens showing slightly higher tensile stress values indicating improve strain resistance. This is expected as the load is carried along the printed lines where more compact material for high infill leads to higher 3D-printed part strength. Similarly to PLA specimens of the same standard, the difference in stress response between 20% and 60% was less than from 60% to 100%.

Figure 3 provides a comparison of a representative stress-strain curve for PLA/TPU specimens type and infill percentage. This comparison indicates an improvement in stress-strain performance in respect to infill percentage for both PLA and TPU. It can be noted that TPU specimens showed considerably lower tensile stress level as well a different profile of stress-strain curves to that of PLA. Furthermore, the initial linear portion of the stress-strain curves were less steep for soft TPU with different infill compared to specimens based on semi-rigid PLA. Highly flexible polymers like TPU do not follow a clear linear profile and are able to have large deformation prior to fracture (500%).

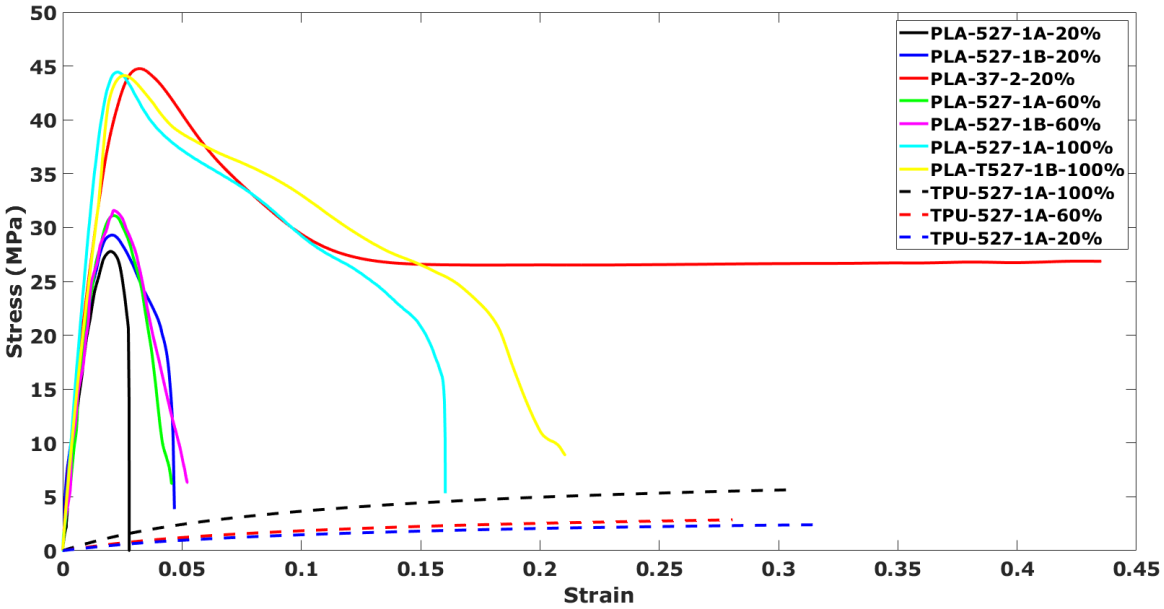

Figure 3 Tensile Stress-Strain curves of PLA and TPU95A with 20%,60%,100% infill.

3.2. Compression test of PLA

Two different sizes of PLA specimens were used to investigate the impact of the infill percentage and dimensions, on the compressive behaviour of 3D printed PLA. The compressive response of PLA (with 20%, 60%, and 100% infill) are compared and illustrated in Figure 4. The yield stress of PLA differed considerably based on infill percentage. The 10 mm diameter, specimens (D10) of 100% infill showed the highest yield stress of 54.20±0.3 MPa, whilst the 20% infill specimens had the lowest yield stress of 25.95±0.5 MPa. Cavities and voids in low infill specimens are likely to have a significant effect in specimen strength (Subeshan, et al. 2018). In addition, smaller differences were observed in the elastic phase. The compressive modulus of PLA specimens increased with the infill percent for D10 specimens changing from 1.0 GPa for 20% infill, to 1.37 GP for 60% and 2.26 GPa for 100% infill.

The compressive response of the small sized specimens i.e. diameter of 5mm (D5), was almost identical for both 20% and 60% infill specimens suggesting that the resulting specimens were in fact of similar resulting infill and structure. This is likely a result of the limitations of the manufacturing method. The consistency of the compressive modulus for samples with small size is in agreement with some relevant literature (Guessasma, et al. 2016). The stress response of the D5 specimens (20% and 60% infill) was similar to the D10 100% infill specimens after around 30% strain, probably as a result of densification.

The results arguably highlight that the selection of geometry dimensions and infill of the 3D printed parts had a crucial impact on the resulting strength and stiffness.

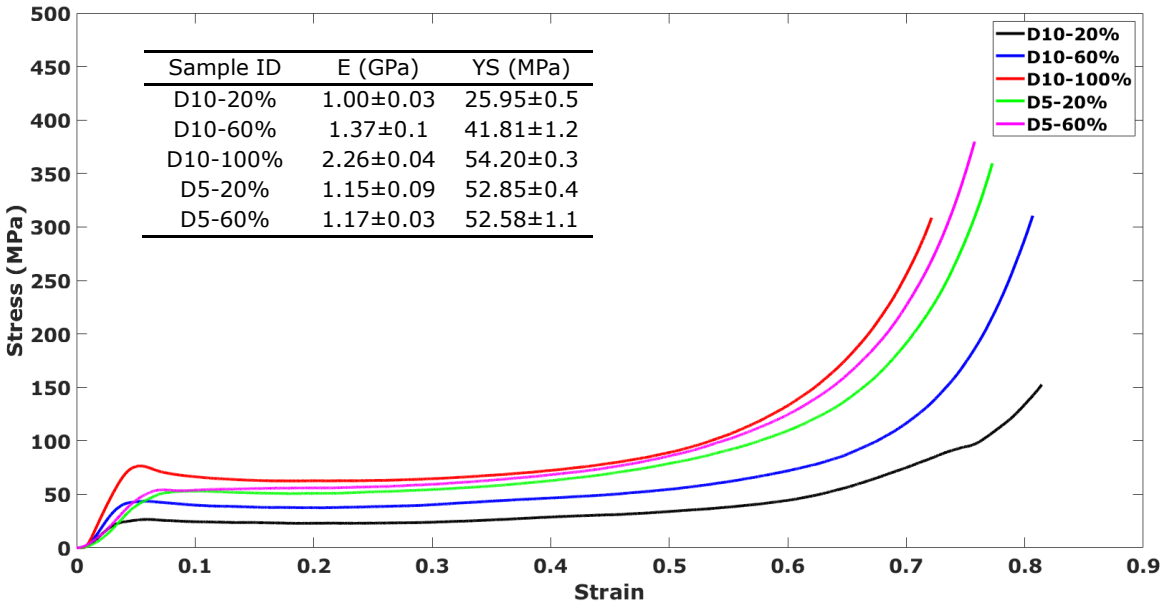

Figure 4 Compression Stress-Strain curves of PLA with 20%,60%,100% infill.

4. Discussion-Conclusion

The effect of infill percentage on the compressive and tensile properties of PLA and TPU specimens manufactured with an ultimaker 3 printer was studied. Specimens made under settings for 20%, 60%, and 100% infill were analysed. Tensile specimens were made following ISO standard recommendations. Tests were carried out to determine the mechanical response of the PLA and TPU printed specimens. Stress-Strain curves are provided as guidance for designing functional parts under the settings used in this study. The study was limited to compressive and tensile tests. Further studies on mechanical properties (e.g. shear, bending) would provide with useful additional information and could be the topic of future work.

The results suggest that compressive and tensile properties of 3D printed parts, may significantly vary depending on the infill percentage settings and dimensions. Whilst infill percentage settings might be constant, the resulting material properties might vary depending on the size of the specimen. This consideration can be important when designing functional parts for 3D printing. 3D printer resolution limitations and the ratio of outline wall thickness to part cross section may significantly affect the resulting properties. Perhaps further infiltration of 3D printing into relevant commercial activity could drive the development of industry standards and generate comprehensive guidelines. Data bases linking mechanical properties with printing parameters and design dimensions, or built-in software tools that estimate the distribution of properties across a design could be potential approaches in assisting designers and engineers in their decision process.

Data Availability Statement

The raw/processed data required to reproduce these findings cannot be shared at this time due to technical and time limitations. Data are available upon request and within a reasonable period.

Reference:

Avérous, L., 2008, Polylactic acid: synthesis, properties and applications. *In:* Polylactic acid: synthesis, properties and applications. *Monomers, polymers and composites from renewable resources.* Elsevier, 2008, pp. 433-450.

Bin Ishak, I., Fleming, D. and Larochelle, P., 2019. Multiplane fused deposition modeling: a study of tensile strength. *Mechanics Based Design of Structures and Machines,* 47 (5), 583-598.

Brenken, B., et al., 2018. Fused filament fabrication of fiber-reinforced polymers: A review. *Additive Manufacturing,* 21, 1-16.

Cantrell, J.T., et al., 2017. Experimental characterization of the mechanical properties of 3D-printed ABS and polycarbonate parts. *Rapid Prototyping Journal,* .

Chacón, J.M., et al., 2017. Additive manufacturing of PLA structures using fused deposition modelling: Effect of process parameters on mechanical properties and their optimal selection. *Materials & Design,* 124, 143-157.

Chen, Q., et al., 2017. 3D printing biocompatible polyurethane/poly (lactic acid)/graphene oxide nanocomposites: anisotropic properties. *ACS Applied Materials & Interfaces,* 9 (4), 4015-4023.

Compton, B.G. and Lewis, J.A., 2014. 3D-printing of lightweight cellular composites. *Advanced Materials,* 26 (34), 5930-5935.

Dal Maso, A. and Cosmi, F., 2018. Mechanical characterization of 3D-printed objects. *Materials Today: Proceedings,* 5 (13), 26739-26746.

Davis, J.R., 2004. *Tensile testing.* ASM international.

de Leon, A.C., et al., 2016. High performance polymer nanocomposites for additive manufacturing applications. *Reactive and Functional Polymers,* 103, 141-155.

Ebel, E. and Sinnemann, T., 2014. Fabrication of FDM 3D objects with ABS and PLA and determination of their mechanical properties. *RTejournal,* 2014 (1).

Fernández-Vicente, M. and Conejero, A., 2016. Suitability study of desktop 3d printing for concept design projects in engineering education. *INTED2016 Proceedings,* , 4485-4491.

Guessasma, S., et al., 2016. Anisotropic damage inferred to 3D printed polymers using fused deposition modelling and subject to severe compression. *European Polymer Journal,* 85, 324-340.

Guo, N. and Leu, M.C., 2013. Additive manufacturing: technology, applications and research needs. *Frontiers of Mechanical Engineering,* 8 (3), 215-243.

Han, T., et al., 2019. 3D Printed Sensors for Biomedical Applications: A Review. *Sensors,* 19 (7), 1706.

Hofmann, G.O., Kluger, P. and Fische, R., 1997. Biomechanical evaluation of a bioresorbable PLA dowel for arthroscopic surgery of the shoulder. *Biomaterials,* 18 (21), 1441-1445.

Hohimer, C., et al., 2017. 3D printed thermoplastic polyurethane with isotropic material properties. *In: Behavior and Mechanics of Multifunctional Materials and Composites 2017,* International Society for Optics and Photonics, pp. 1016511.

Kim, H., et al., 2017. Experimental study on mechanical properties of single-and dual-material 3D printed products. *Procedia Manufacturing,* 10, 887-897.

Li, H., et al., 2018. The effect of process parameters in fused deposition modelling on bonding degree and mechanical properties. *Rapid Prototyping Journal,* .

Mani, M., Lyons, K.W. and Gupta, S.K., 2014. Sustainability characterization for additive manufacturing. *Journal of Research of the National Institute of Standards and Technology,* 119, 419.

Muth, J.T., et al., 2014. Embedded 3D printing of strain sensors within highly stretchable elastomers. *Advanced Materials,* 26 (36), 6307-6312.

Pahonie, R.C., et al., 2017. Experimental characterisation of the mechanical properties of lightweight 3D printed polymer materials for biomechanical application in ankle-foot orthosis. *Materiale Plastice,* 54 (2), 396.

Parandoush, P. and Lin, D., 2017. A review on additive manufacturing of polymer-fiber composites. *Composite Structures,* 182, 36-53.

Pei, E., et al., 2015. The impact of process parameters on mechanical properties of parts fabricated in PLA with an open-source 3-D printer. *Rapid Prototyping Journal,* .

Popescu, D., et al., 2018. FDM process parameters influence over the mechanical properties of polymer specimens: A review. *Polymer Testing,* 69, 157-166.

Qattawi, A., Alrawi, B. and Guzman, A., 2017. Experimental optimization of fused deposition modelling processing parameters: a design-for-manufacturing approach. *Procedia Manufacturing,* 10, 791-803.

Rohde, S., et al., 2018. Experimental characterization of the shear properties of 3D–printed ABS and polycarbonate parts. *Experimental Mechanics,* 58 (6), 871-884.

Sha, L., et al., 2016. Polylactic acid based nanocomposites: Promising safe and biodegradable materials in biomedical field. *International Journal of Polymer Science,* 2016.

Song, Y., et al., 2017. Measurements of the mechanical response of unidirectional 3D-printed PLA. *Materials & Design,* 123, 154-164.

Subeshan, B., et al., 2018. Investigating compression strengths of 3D printed polymeric infill specimens of various geometries. *In: Nano-, Bio-, Info-Tech Sensors, and 3D Systems II,* International Society for Optics and Photonics, pp. 105970N.

Tao, Y., et al., 2019. Application of a thermoplastic polyurathane/polylactic acid composite filament for 3D-printed personalized orthosis. *Materiali in Tehnologije,* 53 (1), 71-76.

Tao, Z., et al., 2017. Design and optimization of prosthetic foot by using polylactic acid 3D printing. *Journal of Mechanical Science and Technology,* 31 (5), 2393-2398.

Torres, J., et al., 2016. An approach for mechanical property optimization of fused deposition modeling with polylactic acid via design of experiments. *Rapid Prototyping Journal,* .

Torres, J., et al., 2015. Mechanical property optimization of FDM PLA in shear with multiple objectives. *Jom,* 67 (5), 1183-1193.

Treiser, M., et al., 2013, Degradable and resorbable biomaterials. *In:* Degradable and resorbable biomaterials. *Biomaterials Science: An Introduction to Materials: Third Edition.* Elsevier Inc., 2013, pp. 179-195.

Tymrak, B.M., Kreiger, M. and Pearce, J.M., 2014. Mechanical properties of components fabricated with open-source 3-D printers under realistic environmental conditions. *Materials & Design,* 58, 242-246.

Wu, W., et al., 2015. Influence of layer thickness and raster angle on the mechanical properties of 3D-printed PEEK and a comparative mechanical study between PEEK and ABS. *Materials,* 8 (9), 5834-5846.

Yao, T., et al., 2019. A method to predict the ultimate tensile strength of 3D printing polylactic acid (PLA) materials with different printing orientations. *Composites Part B: Engineering,* 163, 393-402.